SSRG International Journal of Mechanical Engineering
ISSN: 2348–8360 / https://doi.org/10.14445/23488360/IJME-V10I7P101

Volume 10 Issue 7, 1-13, July 2023

Original Article

Numerical and Experimental Examination of Novel Delta Cut Winglet

Vaibhav Pandey[1], Kaustubh Pawar[1], Shaunak Joshi[1], Sudesh Kadam[1], Harshad Deshpande[1]

[1]*Department of Mechanical Engineering, PES's Modern College of Engineering, Pune, Maharashtra, India.*

Received: 26 April 2023 Revised: 18 June 2023 Accepted: 10 July 2023 Published: 31 July 2023

Abstract *- Details of a numerical and experimental investigation on the heat transfer characteristics for three-dimensional turbulent flows in a rectangular duct with punched Delta Cut Winglet are presented in the present article. The aim of the study is to examine the influence of the winglet shape, attack angles of 0^0, 30°, 45°, 60°, 90^0 on different patterns viz., Inline and Staggered, Height of Perforation viz., H/2, H/3 and H/4, Diameter of Perforation 2.5mm, 3.25mm and 4mm on the Nusselt Number Ratio, Friction Factor Ratio and Thermal Enhancement Factor(TEF) for Reynolds numbers ranging from 12180.699 to 48722.796. The results are compared with turbulent flows' flow and heat transfer characteristics in rectangular ducts without winglets. Numerical results predict an augmentation in the thermal performance of the rectangular duct flows with winglets. Experimental results validate the results obtained in numerical analysis. By numerical analysis, we concluded that the ratio of Nusselt Number is more while the ratio of Friction Factor is less at an attack angle of 0^0 compared to 30^0, 45^0, 60^0 & 90^0. By Numerical Analysis, we concluded that the Thermal Enhancement Factor is more at an attack angle of 0^0 than 30^0, 45^0, 60^0 & 90^0. By Numerical Analysis, we concluded that the ratio of Nusselt Number is more while the ratio of Friction Factor is less, which complies with TEF is more when the height of perforation from the base of the winglet is H/2 as compared to H/3 and H/4. The values of Nu/Nu_0 is 1.6248, and f/f_0 is 0.8974. The highest value of TEF achieved is 1.6844.*

Keywords *- Heat transfer, Rectangular duct, Thermal Enhancement Factor, Turbulent flow, Winglets.*

1. Introduction

Thermal performance improvements techniques such as fins, vortex generators (VGs) such as wing, winglet, baffle, groove and ribs have been used to enhance the thermal performance of compact heat exchangers for various applications in chemical, electronic, automobile, and smelting industries, internal cooling systems of gas turbines, electronic equipment cooling and many others [1-2]. Early work in this area was reported in 1974 by Edwards and Alker and in 1986 by Turk and Junkhan. Introducing VGs aims to change the flow structure and increase three-dimensional mixing by inducing transverse/longitudinal vortices or/and swirl flow. Introducing VGs regularly in compact heat exchangers lead 10 to interruption and breakage of the hydrodynamic and thermal boundary layer, thereby enhancing the heat transfer. [3] Show that the experiments were performed for a single row by increasing the number of the vortex generators in the row (2, 4, 6, and 8) so that the transverse pitch ratios were 0.50, 0.25, 0.16, and 0.12. The highest increases in *Nu* compared with the smooth channel were approximately 21%, 36%, 44%, and 44% for *RT* = 0.50, 0.25, 0.16, and 0.12 at *Re* = 5000, respectively. [4] Shows that various cases of RWVGs without and with circular punched holes (1, 2, 4, and 6 holes) are considered. RWVG with 1-hole, 2-hole, 4 holes, and 6 holes exhibits an appreciable reduction in friction factor which is about 3.8%, 4.4%, 11% and 13.81%, respectively. [5] Comparisons based on heat transfer and flow resistance characteristics have been drawn between punched and non-punched cases of rectangular winglets with holes for all the configurations. Plate-punching proved to be advantageous in the upstream location when considering thermal characteristics, whereas common flow up at the upstream location and common flow down at the downstream location proved to be advantageous in terms of pressure drop obtained. [7] Shows that concave and convex curved delta winglet VGs in a channel of the plate heat exchanger under laminar flow are studied and compared with the normal plane delta winglet VG to optimize the shape of VGs. The concave curved VG has excellent heat transfer performance than the convex curved VG. [8] Shows that the thermal performance of a heat exchanger duct with punched winglets (PWs) mounted on the upper duct wall has been examined for Reynolds number (Re) ranging from 4100 to 25,500. It concludes that for experimental results, heat transfer enhancement by WVGs is superior to those by PWs, and the DW performs higher than the EW. [9] In this paper, three-dimensional numerical simulations of VGs are performed to analyze the heat transfer enhancement and the flow resistance in a rectangular channel with two-row rectangular vortex generators with and without a hole at the Re from 214 to 10,703. Finally, compared to the thermo hydraulic performance, it can be seen that the rectangular vortex generators with a hole perform better than the rectangular vortex generators without a hole. [10] This paper presents an experimental study of detailed heat transfer and flow field characteristics in a rectangular duct having different types of truncated prismatic ribs on the bottom surface. It concludes that, among the studied rib configurations, truncated prismatic rib with *ep*/*e* = 1/4 yields the highest overall averaged augmentation Nusselt number, about 25.15% higher than those with the square ribs at

Re=58,850. [12] A numerical investigation of the heat transfer characteristics for three-dimensional laminar flows in a rectangular duct with four different winglets is presented here. The four winglet shapes are the conventional delta winglet and three new winglets, namely, arrow, delta-cut and X winglet. Delta and delta-cut winglets have a detrimental effect when the flow attack angle is increased. The arrow winglet has no significant effect, and the X winglet's thermal performance improves with an increase in flow attack angle. [13] Heat transfer and flow friction measurements were conducted for a fully developed turbulent flow in a rectangular duct with its bottom wall ribbed with three different rib geometries (semi-circular, rectangular and hybrid ribs of the two). The Nusselt number enhancement ratio was obtained between 1.3 and 2.14, corresponding to a friction factor ratio of 1.8 and 4.2. [14] A three-dimensional numerical simulation is being carried out to study the thermo-hydraulic performance of curved rectangular winglet vortex generators with elliptical punched holes. The best thermo-hydraulic performance was obtained for the staggered arrangement with a Nusselt number (Nu) increase of about 54% compared to the smooth plate. [16] Shows that the effects of attack angle (b = 15 deg, 30 deg, 45 deg, and 60 deg), pitch (P = 1D, P = 2D, P = 3D, and P = 4D) and Reynolds numbers ranging from 6000 to 20,000 of delta-winglet vortex generators on heat transfer and fluid flow are examined in detail. It concludes that the delta-winglet vortex generators significantly improve the thermal-hydraulic performance of circular tubes with a modest pressure drop penalty. The Nusselt number increase with the increase of attack angle, and the increased tendency decreases with the increase of attack angle. [17] Shows that the effect of inline and staggered arrangement with curved rectangular winglet vortex generators on a flat plate for heat transfer and friction factor characteristics is studied numerically and compared with the performance of a smooth plate. Best thermo-hydraulic performance was obtained for a staggered arrangement with a Nusselt number (Nu) increase of about 54% compared to the smooth plate. [18] Shows that the effects of two new types of LVGs, i.e., the common-flow-up rectangular winglet combined with an elliptical pole (Case E) and the common-flow-up delta winglet combined with an elliptical pole (Case F), on flow and heat transfer characteristics in a rectangular channel are investigated in detail by three-dimensional CFD numerical simulations. It concludes that, at the same Reynolds number, the effect of heat transfer enhancement is concluded such that Case E > Case C > Case A > Case F > Case D > Case B > Case G. Case E provides the best heat transfer enhancement. [19] Shows that numerical investigation on heat transfer behaviours in a constant heat-fluxed round tube inserted with winglet vortex generators is conducted. Air as the working medium flows through the tube for Reynolds numbers (Re) between 4000 and 20,000. The numerical results show that the Nusselt number (Nu) and friction factor (*f*) of the tube inserts are enhanced with increasing *B*R values. The Nu for the inserted tube is about 1.8-2.7 times above that for the smooth tube, while the *f* is around 4.5-11 times higher. [20] shows that the angle of attack of a pair of delta-winglet-type VGs mounted behind each tube is varied between b = +90 and -90. Three circular tube rows with inline and staggered tube arrangements are investigated for Reynolds numbers from 200 to 1200. The results obtained show that the use of delta-winglets as heat transfer enhancement elements increases the performance of plate-fin and- tube heat exchangers.

2. Mathematical Model

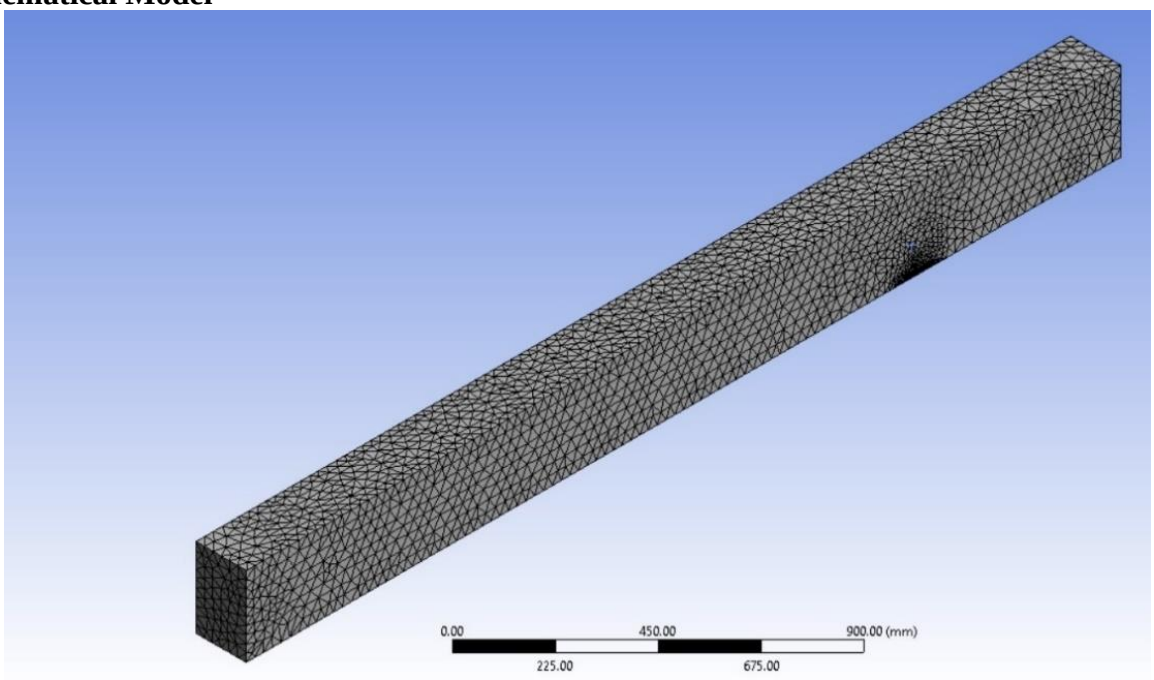

Fig. 1 Geometry mesh

Table 1. Types of mesh and grids

Sr. No.	Geometry	Nodes	Mesh	Grid
1.	Flat Plate	30211	Unstructured	Hexahedral
2.	Delta Cut Winglet (Attack Angle = 0^0, Pattern: Staggered)	51907	Unstructured	Hexahedral
3.	Delta Cut Winglet with Perforation (Height of Perforation = H/2)	42868	Unstructured	Hexahedral

Table 2. Different boundary conditions

Sr. No.	Boundary Conditions	Value
1.	Inlet Velocity	V=1 m/s,2 m/s,3 m/s,4 m/s
2.	Outlet Gauge Pressure	0 Pa
3.	Adiabatic Surface	q=0 W/m^2
4.	Heated Surface	q=643.0868 W/m^2, 2,572.8987 W/m^2

2.1. Geometries

2.1.1. Flat Plate

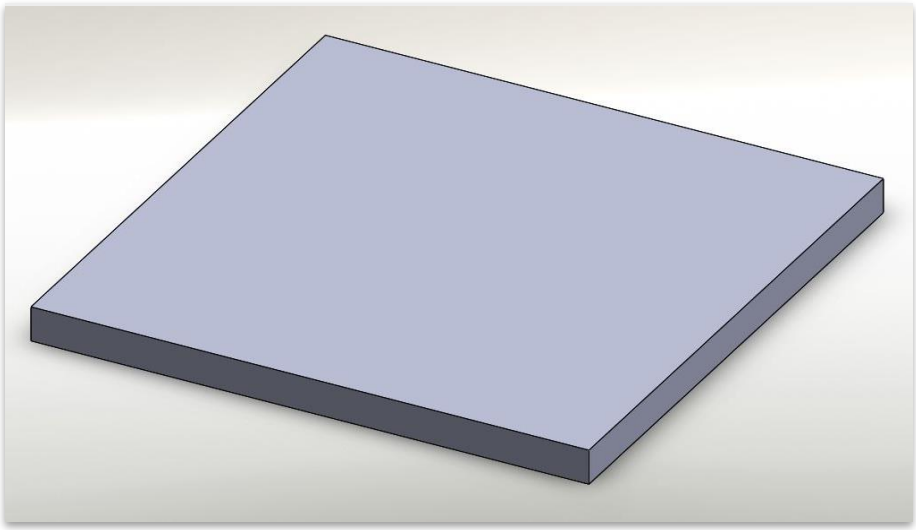

Fig. 2 Geometry

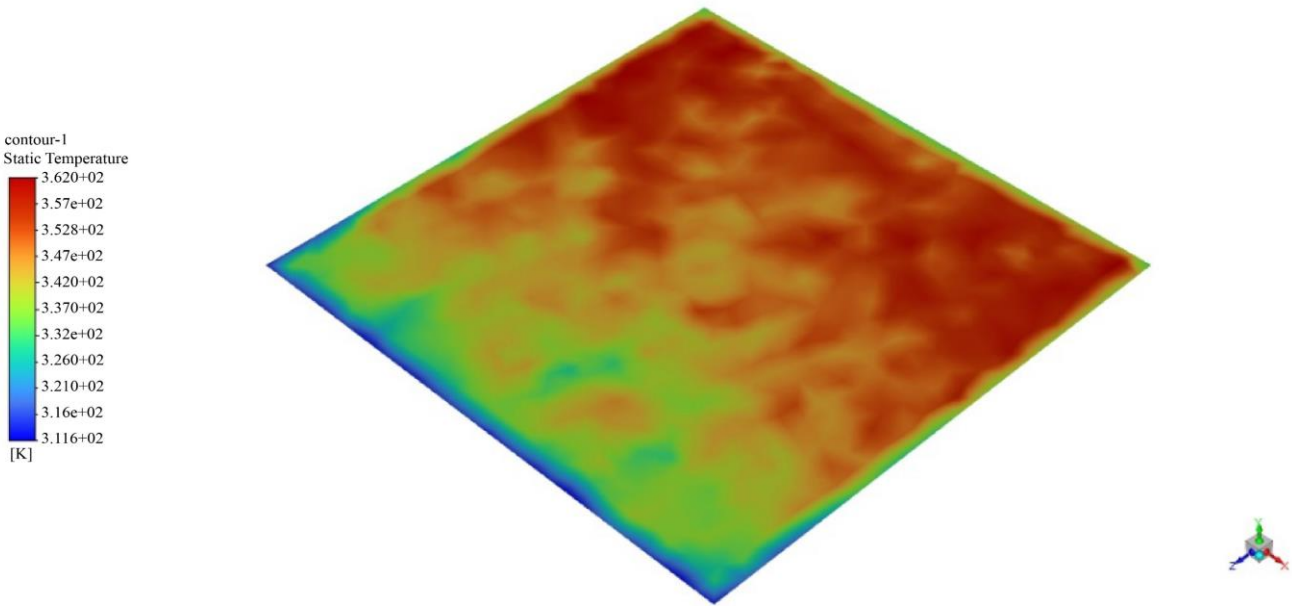

Fig. 3 Temperature contour

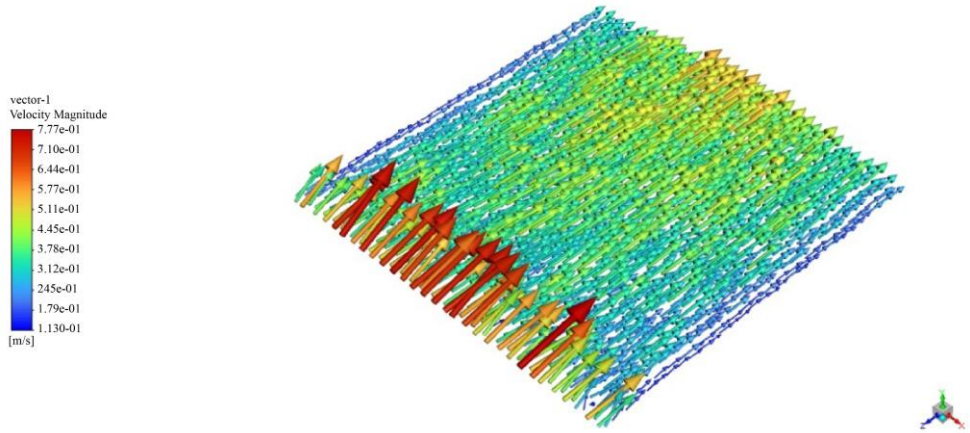

Fig. 4 Velocity vector

We analyzed the flat plate with dimensions of 150mm×150mm×10mm for velocities ranging from 1m/s to 4m/s and heat inputs of 15W and 60W to establish a base reference for other geometries. The Reynolds number ranged from 12,180.699 to 48,722.796, the Nusselt number was 73.71604392, the friction factor was 0.0208143, and the surface temperature was 365.7921K.

2.1.2. Delta Cut Staggered (Pitch=47mm)

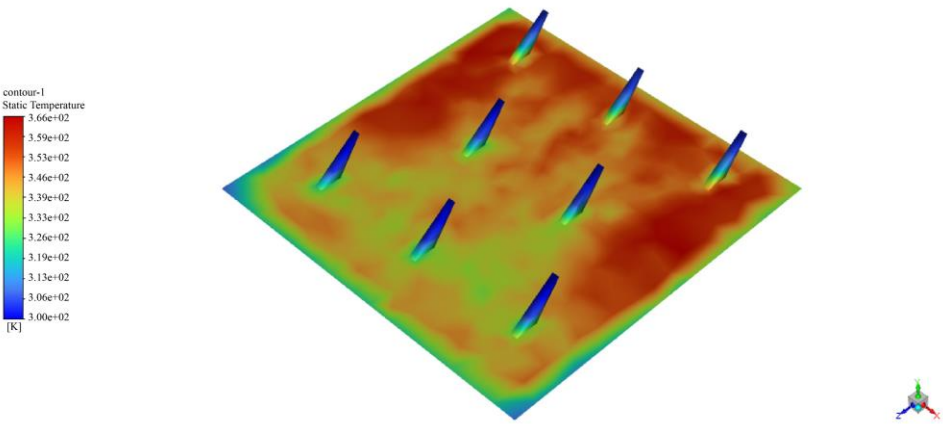

Fig. 5 Temperature contour

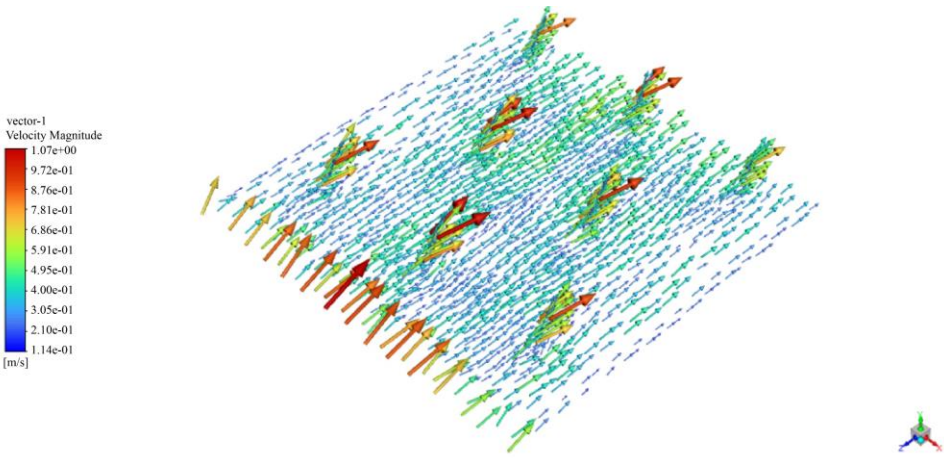

Fig. 6 Velocity vector

We analyzed the flat plate with winglets in a staggered form (pitch=47mm) with dimensions of 20mm×15mm×3mm and an attack angle of 0°. The analysis was conducted for velocities ranging from 1m/s to 4m/s and heat inputs of 15W and 60W. The Reynolds number ranged from 12,180.699 to 48,722.796. The Nusselt number was 97.26889262, the friction factor was 0.0218224, the surface temperature was 348.566K, and the thermal enhancement factor (TEF) was 1.2988.

2.1.3. Delta Cut Staggered (Pitch=27mm)

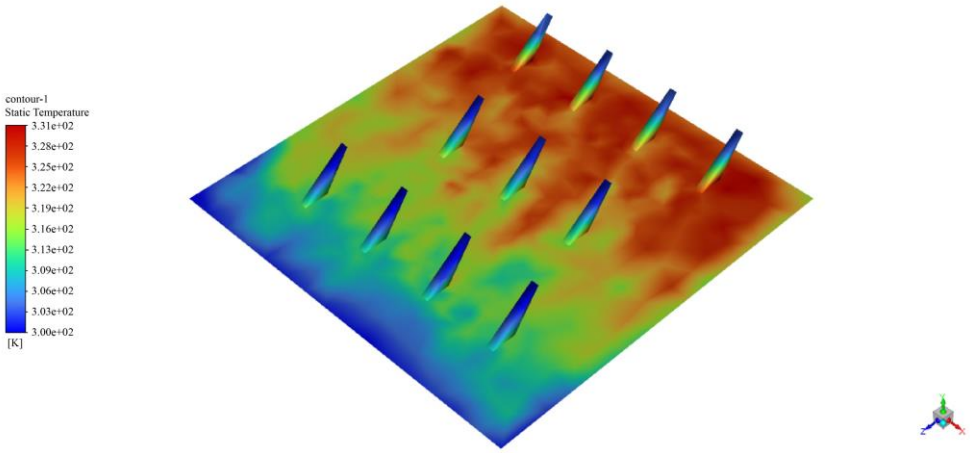

Fig. 7 Temperature contour

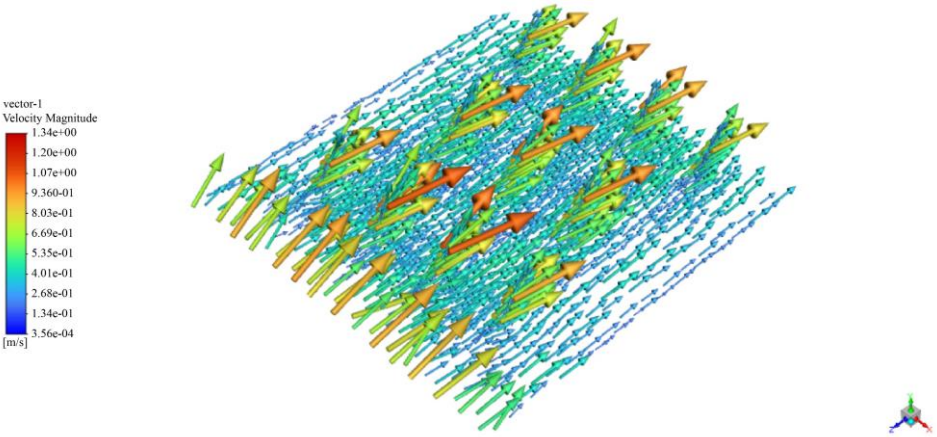

Fig. 8 Velocity vector

We analyzed a flat plate with winglets in a staggered form with a pitch of 27mm. The dimensions of the plate were 20mm×15mm×3mm, and the attack angle was 0°. The analysis covered a velocity range from 1m/s to 4m/s and heat inputs of 15W and 60W. The Reynolds number ranged from 12,180.699 to 48,722.796. The Nusselt number was 97.5705812, the friction factor was 0.02189356, the surface temperature was 347.9488K, and the thermal enhancement factor (TEF) was 1.30148.

2.1.4. Perforation At H/2 (D=2.5mm)

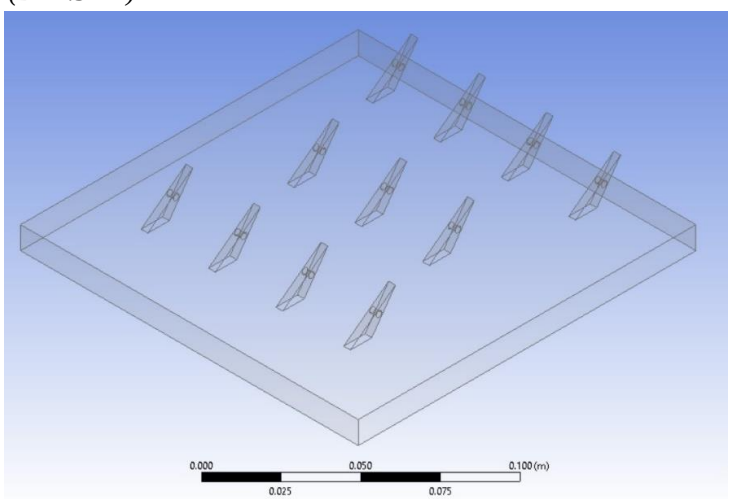

Fig. 9 Geometry

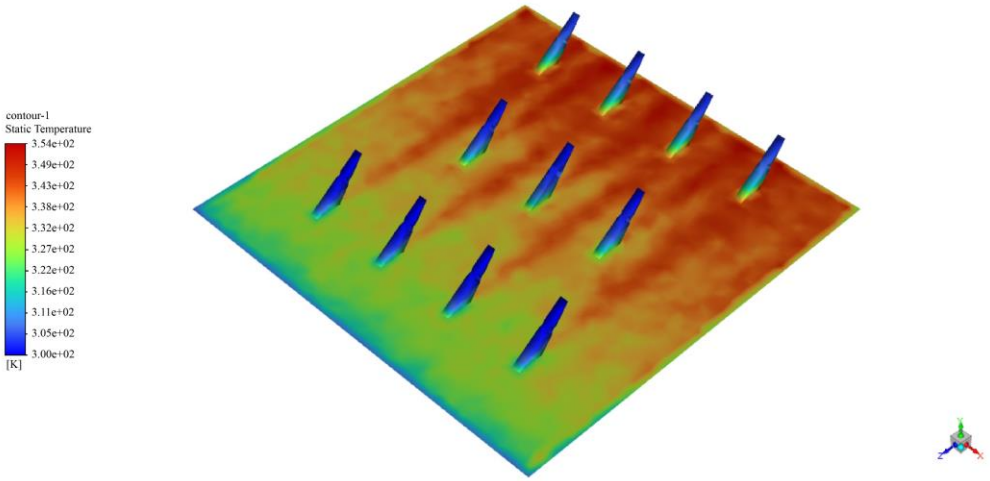

Fig. 10 Temperature contour

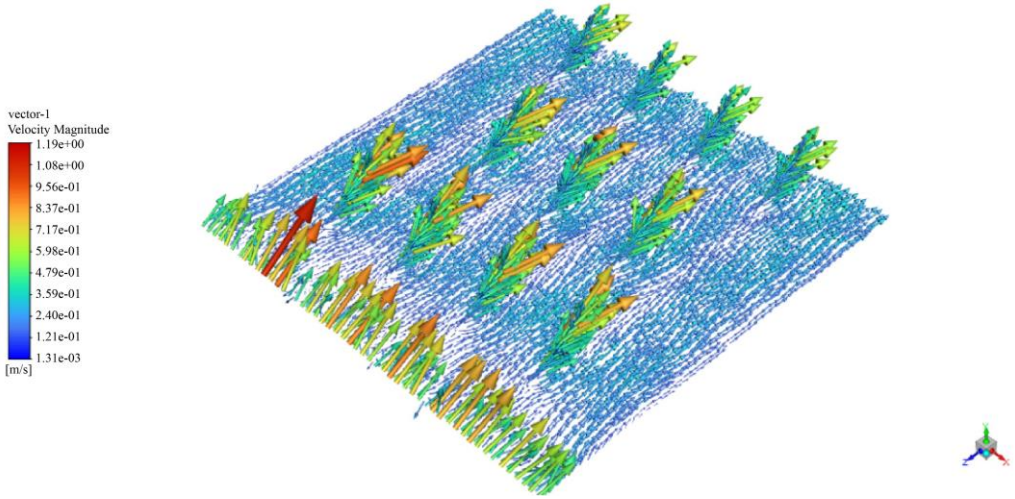

Fig. 11 Velocity vector

We have analyzed a flat plate with winglets in a staggered form (pitch=27mm) with dimensions of 20mm×15mm×3mm. The plate has an attack angle of 0° and a perforation at a height of H/2 from the base, with a diameter of 2.5mm. The analysis covered velocities ranging from 1m/s to 4m/s and heat inputs of 15W and 60W. The Reynolds number ranged from 12,180.699 to 48,722.796. The Nusselt number was 124.308292, the friction factor was 0.0190946, the surface temperature was 339.0601K, and the thermal enhancement factor (TEF) was 1.73549.

2.2. Finalized Geometry

Table 3. Parameters of finalized geometry

Sr. No.	Parameter	Value
1	Pattern	Staggered
2	Attack Angle	0^0
3	Pitch	27mm
4	Perforation Height	H/2
5	Perforation Diameter	2.5mm

3. Setup of Experiment

3.1. Experimental Setup

A heater plate with dimensions of 150mm×150mm is clamped to an aluminium flat plate of the same dimensions (150mm×150mm) and 10mm thickness. The aluminium plate provides heat to the system. Both plates are placed inside a duct. The heater plate is connected to a control panel, which allows for the control of heat input. Eight thermocouples are connected to the plate to measure its surface temperature. A blower, connected to a motor, runs the fan. The velocity of the air can be controlled using the inlet valve. The blower is connected to the duct. The fan facilitates the airflow, which helps dissipate the heat from the plate. The surface temperature of the plate can be determined by monitoring the thermocouples connected to the control panel.

3.2. Procedure

We fixed eight thermocouples on the flat plate and placed them inside the duct at a distance of 650mm from the duct outlet. The other ends of the thermocouples were connected to the control panel using connectors. We connected the heater plate to the control panel using a three-pin connector to provide heat to the plate. Then, we started the control panel and set the wattage to 60W. After providing the heater input, we started the blower and maintained a velocity of 4m/s by measuring the air velocity with an anemometer. We noted the temperature of each thermocouple by rotating the selector present on the control panel at intervals of 10 minutes until it reached a steady state. We repeated the same procedure for velocities of 3m/s, 2m/s, and 1m/s.

Additionally, we repeated the entire procedure for a wattage of 15W. Next, we affixed all 11 winglets onto the flat plate in a staggered form, following the pattern of 4:3:4, using Araldite. We repeated the same procedure for the flat plate and recorded all the readings.

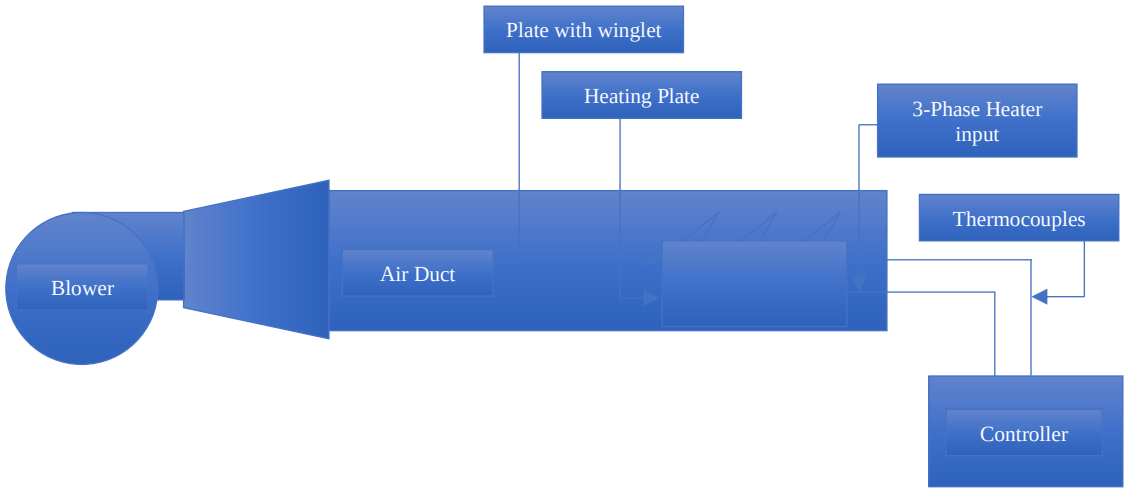

Fig. 12 Experimental setup block diagram

Fig. 13 Test with winglet

4. Data Reduction

4.1. Reynolds Number (Re)

The Reynolds number is a dimensionless parameter used in fluid dynamics to characterize the flow regime of fluid around an object or within a conduit. The Reynolds number (Re) is defined as the ratio of inertial forces to viscous forces within a fluid flow. It is calculated using the following formula:

$$Re = \frac{\rho V L}{\mu}$$

4.2. Nusselt Number (Nu)

The Nusselt number is a dimensionless parameter used in heat transfer analysis. It is defined as the ratio of convective heat transfer to conductive heat transfer across a boundary layer with a winglet. It represents heat transfer enhancement due to convection compared to pure conduction. Mathematically, the Nusselt number is expressed as:

$$Nu = \frac{hD_h}{K}$$

4.3. Friction Factor (f)

The friction factor, also known as the Darcy friction factor or Moody friction factor, is a dimensionless parameter used in fluid dynamics to characterize the resistance to flow in a pipe or conduit. It quantifies the pressure loss at the inlet and outlet with the winglet. The equation is as follows:

$$f = \frac{2D}{\rho L V^2} \Delta p$$

4.4. Nusselt Number (Nu_o)

The Nusselt number is a dimensionless parameter used in heat transfer analysis. It is defined as the ratio of convective heat transfer to conductive heat transfer across a boundary layer without a winglet. It represents heat transfer enhancement due to convection compared to pure conduction. Mathematically, the Nusselt number is expressed as:

$$Nu_o = \frac{hD_h}{K}$$

4.5. Friction Factor (f_o)

The friction factor, also known as the Darcy friction factor or Moody friction factor, is a dimensionless parameter used in fluid dynamics to characterize the resistance to flow in a pipe or conduit. It quantifies the pressure loss at the inlet and outlet without a winglet. The equation is as follows:

$$f_o = \frac{2D}{\rho L V^2} \Delta p$$

4.6. Thermal Enhancement Factor (TEF)

The Thermal Enhancement Factor (TEF) for winglets is a parameter used to quantify the improvement in heat transfer performance achieved by the presence of winglets on a surface, such as in heat exchangers or cooling systems. It is a ratio of increase in Nusselt Number to friction factor. It is used to determine whether the flat plate with a winglet is more efficient than the flat plate without a winglet.

$$\text{TEF} = \frac{\text{Nu}/\text{Nu}_o}{\text{f}/\text{f}_o^{1/3}}$$

5. Results and Discussion

5.1. Effect of Flow Velocity on Nusselt No. and Friction Factor Ratio (Numerical Analysis)

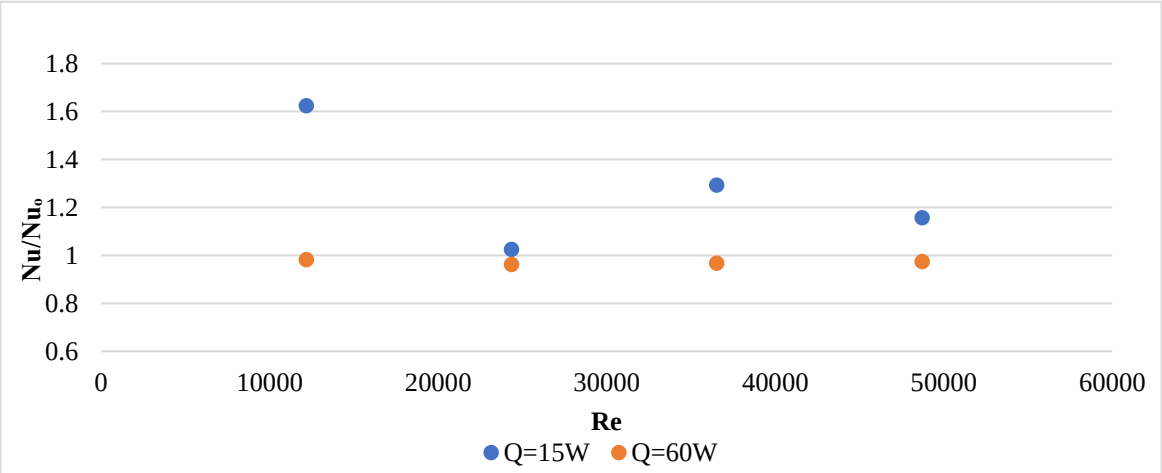

Fig. 14 Nu/Nu_o Vs Re

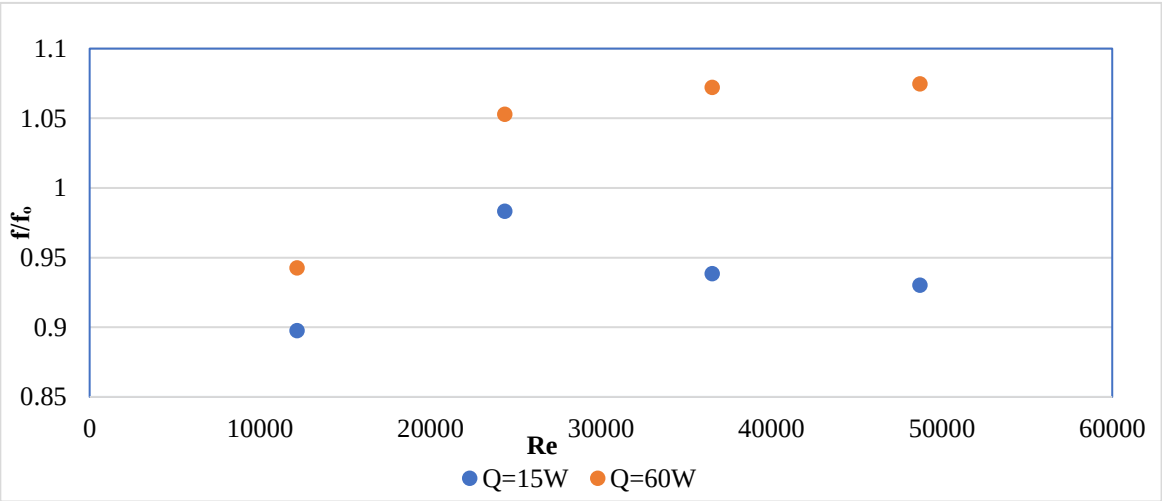

Fig. 15 f/f_o Vs Re

For a greater value of TEF, Nu/Nu_o should be high, as $TEF = \frac{Nu/Nu_o}{(f/f_o)^{1/3}}$. From the graph above, it can be observed that at Q=15W and V=1 m/s, the value of Nu/Nu_o is the highest, which is 1.6248. The minimum value is for Q=60W at V=2 m/s, which is 0.9620. The trend for Q=15W shows a continuous increase-decrease pattern, while the trend for Q=60W is linear.

Similarly, for a greater value of TEF, f/f_o should be low, as $TEF = \frac{Nu/Nu_o}{(f/f_o)^{1/3}}$. From the graph above, it can be observed that at Q=15W and V=1 m/s, the value of f/f_o is the lowest, which is 0.8974. The maximum value is for Q=60W at V=4 m/s, which is 1.0745. The trend for Q=15W first increases and then decreases, while the trend for Q=60W is increasing.

5.2. Effect of Flow Velocity on TEF (Numerical Analysis)

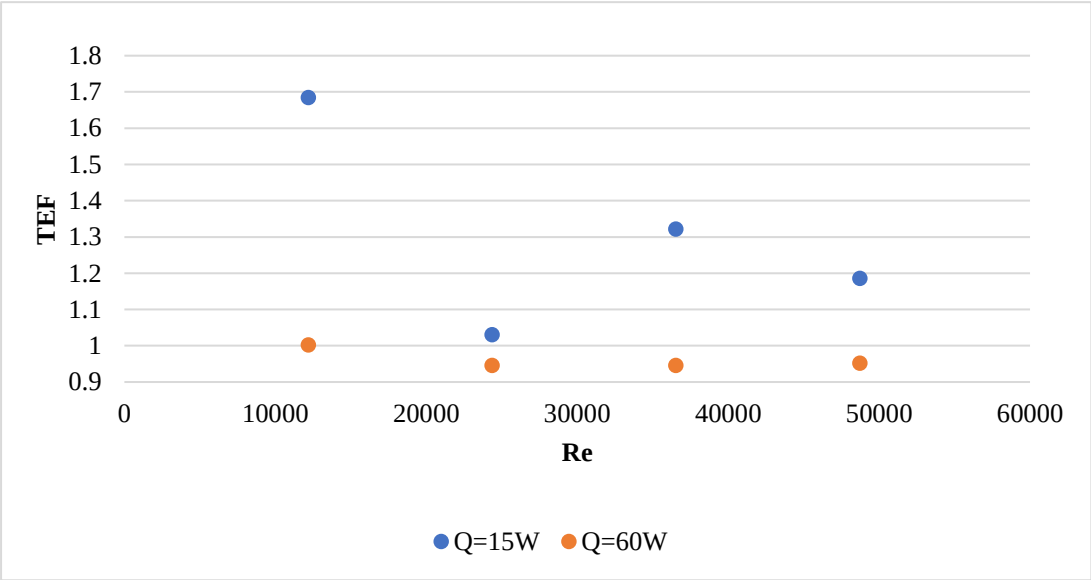

Fig. 16 TEF V/S Re

From the graph above, it can be observed that at Q=15W and V=1 m/s, the value of TEF is the highest, which is 1.6844. The minimum value is Q=60W at V=3 m/s, which is 0.9456. The graph trend for Q=15W is continuously increasing and then decreasing, while the trend for Q=60W is linear.

5.3. Effect of Flow Velocity on Nusselt No. and Friction Factor Ratio (Experimental Analysis)

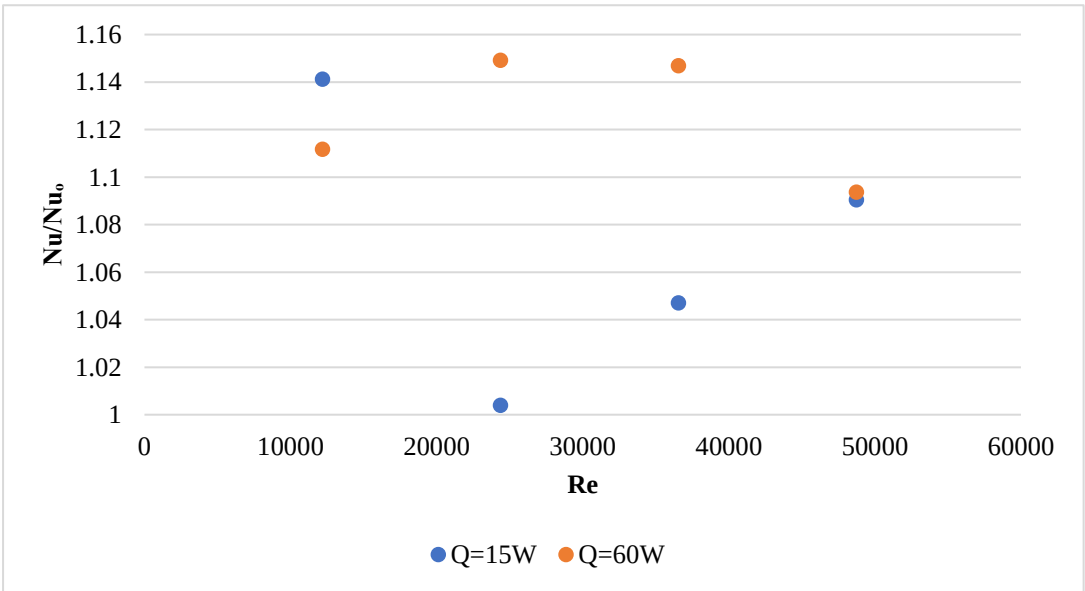

Fig. 17 Nu/Nu_o vs Re

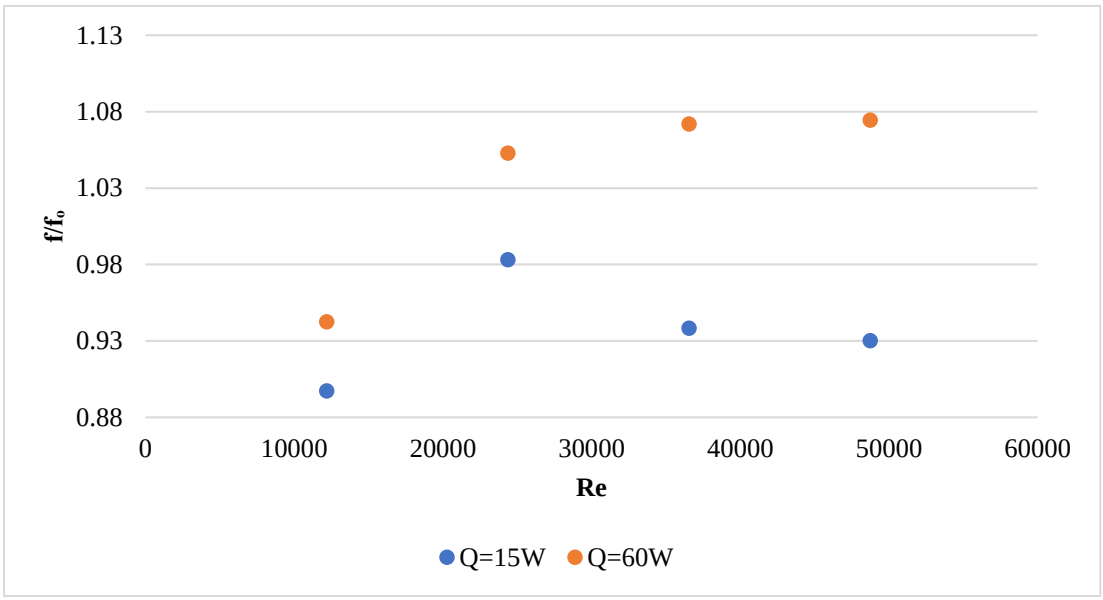

Fig. 18 f/f$_o$ Vs Re

For a greater value of TEF, Nu/Nu$_o$ should be high, as $TEF = \frac{Nu/Nu_o}{(f/f_o)^{1/3}}$. From the graph above, it can be seen that at Q=60W and V=2 m/s, the value of Nu/Nu$_o$ is the highest, which is 1.1491. The lowest value is for Q=15W at V=2 m/s, which is 1.0039. The trend of the graph for Q=15W is first decreasing and then increasing, while the trend for Q=60W is vice versa. Similarly, for a greater value of TEF, f/f$_o$ should be low, as $TEF = \frac{Nu/Nu_o}{(f/f_o)^{1/3}}$. From the graph above, it can be seen that at Q=15W and V=1 m/s, the value of f/f$_o$ is the lowest, which is 0.8974. The highest value is for Q=60W at V=4 m/s, which is 1.0745. The graph trend for Q=15W is first increasing and then decreasing, while the trend for Q=60W is increasing.

5.4. Effect of Flow Velocity on TEF (Experimental Analysis)

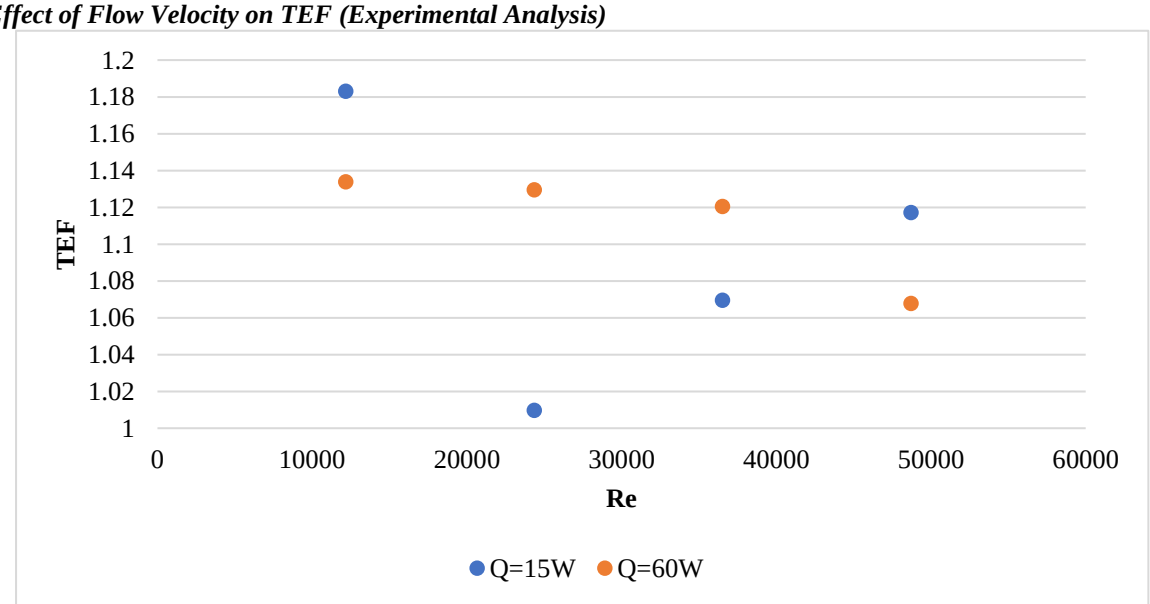

Fig. 19 TEF Vs Re

From the above graph, it can be seen that at Q=15W and V=1 m/s, the value of TEF is the highest, which is 1.1831. The lowest value is for Q=15W at V=2 m/s, i.e., 1.0096. The graph trend for Q=15W first decreases and then increases, while the trend for Q=60W decreases.

5.5. Effect of Other Parameters

5.5.1. Effect of Attack Angle on Nusselt No. and TEF

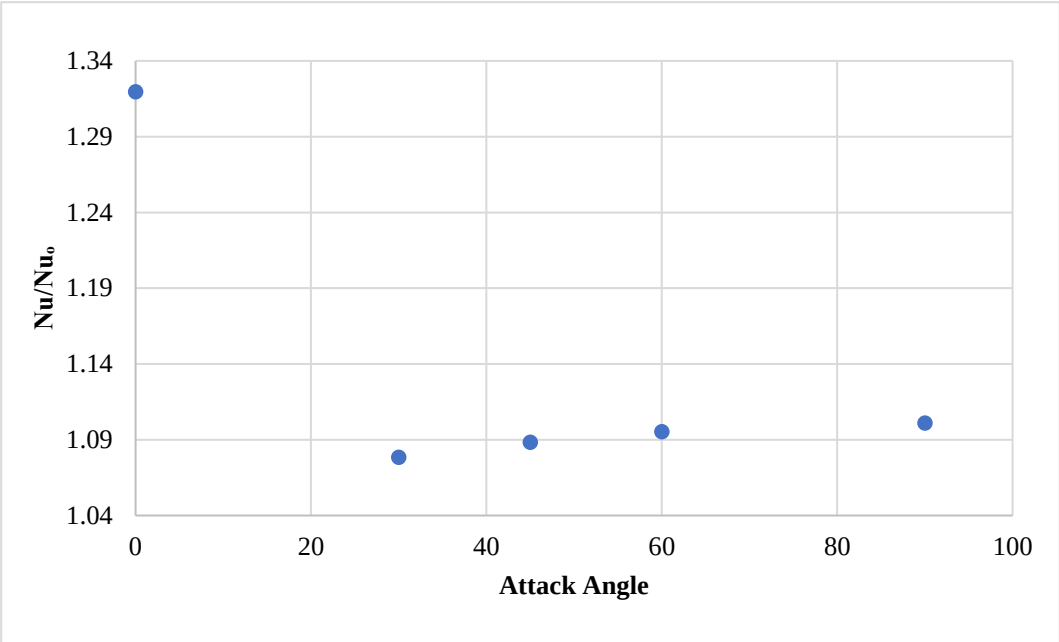

Fig. 20 Nu/Nu$_o$ Vs Attack angle

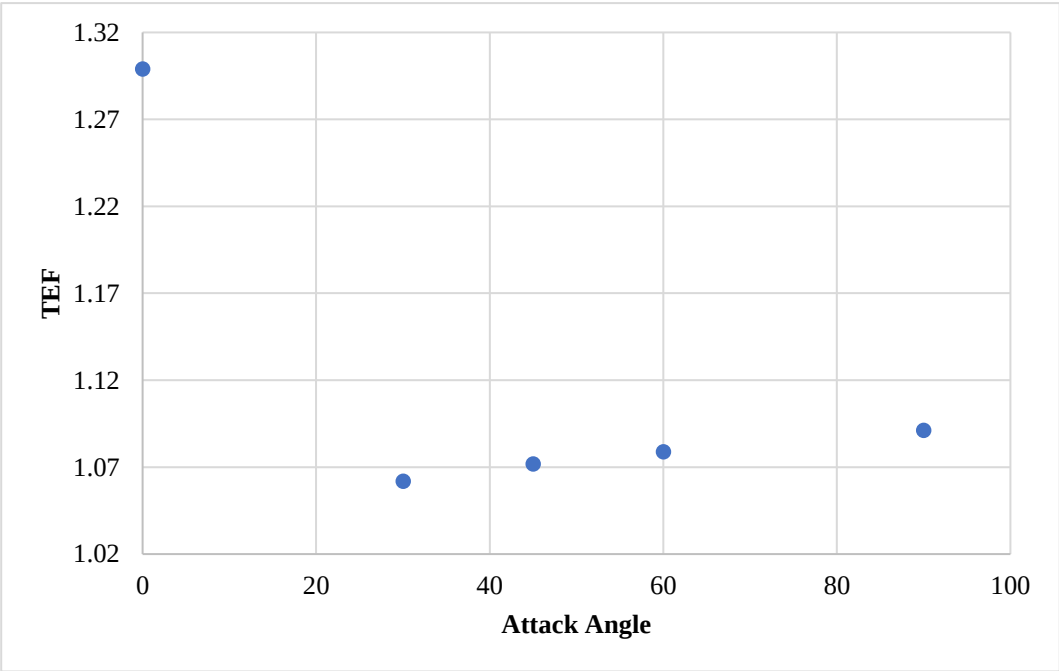

Fig. 21 TEF Vs Attack angle

From the above graph, it can be seen that at an attack angle of 0°, the value of Nu/Nu$_o$ is the highest, which is 1.3195, and the lowest is for an attack angle of 30°, which is 1.0782. For a greater value of TEF, Nu/Nu$_o$ should be high, as $TEF = \frac{Nu/Nu_o}{(f/f_o)^{1/3}}$. From the above graph, it can be seen that at an attack angle of 0°, the value of TEF is the highest, which is 1.2988. The lowest value is for an attack angle of 30°, which is 1.0618.

5.5.2. Effect of Height of Perforation on Nusselt No and TEF

From the above graph, it can be seen that the height of perforation at H/2 has the highest value of Nu/Nu$_o$, which is 1.6648. Its lowest value is 1.6405 for inline. For a greater value of TEF, Nu/Nu$_o$ should be high, as $TEF = \frac{Nu/Nu_o}{(f/f_o)^{1/3}}$. From the above graph, it is observed that the height of perforation at H/2 has the highest value of TEF, which is 1.6844. Its lowest value is 1.6688 for inline.

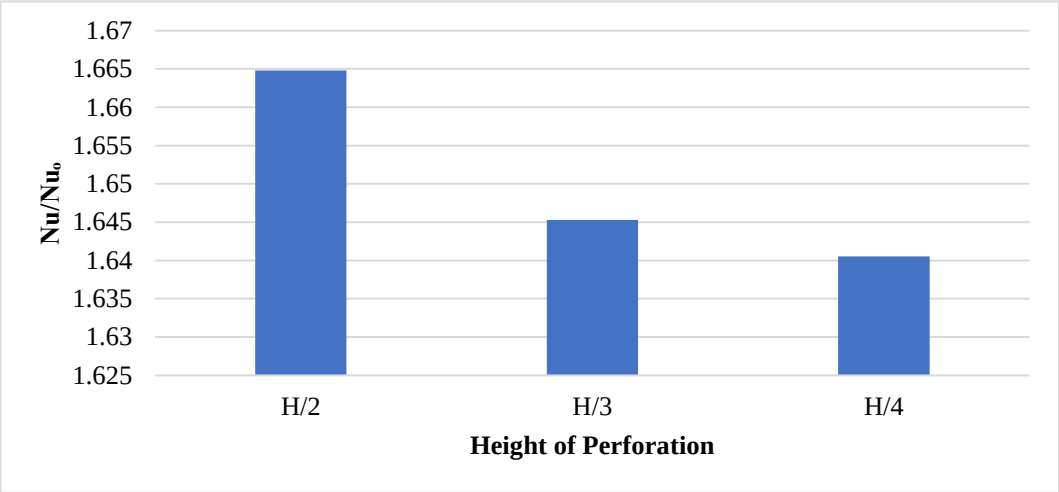

Fig. 22 Nu/Nu₀ Vs Height of perforation

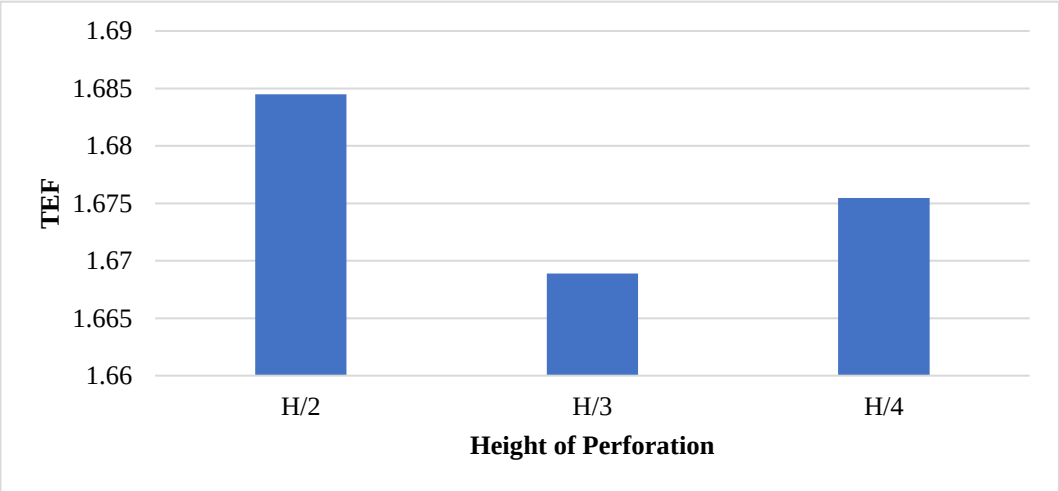

Fig. 23 TEF Vs Height of perforation

6. Conclusion

- Based on numerical analysis, we concluded that the ratio of Nusselt Number is higher at an attack angle of 0° compared to 30°, 45°, 60°, and 90°. Conversely, the ratio of the Friction Factor is lower at an attack angle of 0°. The values of Nu/Nu₀ are 1.3195, and f/f₀ is 1.04843.
- Based on numerical analysis, we concluded that the Thermal Enhancement Factor is higher at an attack angle of 0° compared to 30°, 45°, 60°, and 90°. The value of TEF is 1.2988.
- Based on numerical analysis, we concluded that the ratio of the Nusselt Number is higher while the ratio of the Friction Factor is lower when the height of perforation from the base of the winglet is H/2 compared to H/3 and H/4. The values of Nu/Nu₀ are 1.6248, and f/f₀ is 0.8974.
- Based on numerical analysis, we concluded that the Thermal Enhancement Factor is higher when the height of perforation from the base of the winglet is H/2 compared to H/3 and H/4. The value of TEF is 1.6844.
- Based on experimental analysis, we concluded that the ratio of Nusselt Number is higher while the ratio of Friction Factor is lower for Q=15W at V=1m/s compared to V=2m/s, 3m/s, 4m/s, and Q=60W. The values of Nu/Nu₀ are 1.1412, and f/f₀ is 0.8974.
- Based on experimental analysis, we concluded that the Thermal Enhancement Factor is higher for Q=15W at V=1m/s compared to V=2m/s, 3m/s, 4m/s, and Q=60W. The value of TEF is 1.1831.

References

[1] Harshad Deshpande, Santosh Taji, and Vaijanath Raibhole, "Assessment of Heat Transfer Performance from Modified Horizontal Rectangular Heat Sink Under Forced Convection Dominating Mode of Mixed Convection," *Materials Today: Proceedings*, vol. 47, pp. 5618–5628, 2021. [CrossRef] [Google Scholar] [Publisher Link]

[2] Harshad Deshpande, and Vaijanath Raibhole, "Numerical Assessment of Thermal Performance of Heated Air Duct with Novel Arc Profile Ribs in Non-interrupted Arrangement," *Materials Today: Proceedings*, vol. 63, pp. 6-14, 2022. [CrossRef] [Google Scholar] [Publisher Link]

[3] Mehmet Dogan, and Sait Erzincan, "Experimental Investigation of Thermal Performance of Novel Type Vortex Generator in Rectangular Channel," *International Communications in Heat and Mass Transfer*, vol. 144, p. 106785, 2023. [CrossRef] [Google Scholar] [Publisher Link]

[4] Ashish J Modi, Navnath A Kalel, and Manish K Rathod, "Thermal Performance Augmentation of Fin-and-tube Heat Exchanger using Rectangular Winglet Vortex Generators having Circular Punched Holes," *International Journal of Heat and Mass Transfer*, vol. 158, p. 119724, 2020. [CrossRef] [Google Scholar] [Publisher Link]

[5] Arvind Gupta et al., "Numerical Investigation towards Implementation of Punched Winglet as Vortex Generator for Performance Improvement of a Fin-and-tube Heat Exchanger," *International Journal of Heat and Mass Transfer*, vol. 149, p. 119171, 2020. [CrossRef] [Google Scholar] [Publisher Link]

[6] S. Prathiban, and B. Sivaraman, "Experimental Investigation of Effective Adiabatic Length as A Heat Pipe Heat Exchanger," *International Journal of Engineering Trends and Technology*, vol. 69, no. 6, pp. 43-49, 2021. [CrossRef] [Publisher Link]

[7] KeWei Song et al., "Heat Transfer Characteristics of Concave and Convex Curved Vortex Generators in the Channel of Plate Heat Exchanger under Laminar Flow," *International Journal of Thermal Sciences*, vol. 137, pp. 215–228, 2019. [CrossRef] [Google Scholar] [Publisher Link]

[8] Pongjet Promvonge, and Sompol Skullong, "Enhanced Heat Transfer in Rectangular Duct with Punched Winglets," *Chinese Journal of Chemical Engineering*, vol. 28, no. 3, pp. 660-671, 2020. [CrossRef] [Google Scholar] [Publisher Link]

[9] Zhimin Han, Zhiming Xu, and Jingtao Wang, "Numerical Simulation on Heat Transfer Characteristics of Rectangular Vortex Generators with a Hole," *International Journal of Heat and Mass Transfer*, vol. 126, pp. 993–1001, 2018. [CrossRef] [Google Scholar] [Publisher Link]

[10] Naveen Sharma, Andallib Tariq, and Manish Mishra, "Detailed Heat Transfer and Fluid Flow Investigation in a Rectangular Duct with Truncated Prismatic Ribs," *Experimental Thermal and Fluid Science*, vol. 96, pp. 383–396, 2018. [CrossRef] [Google Scholar] [Publisher Link]

[11] Virendra Bisen, and N. K. Sagar, "A Review on Thermal Performance Analysis for Annular Fins of Various Profiles using Ansys," *SSRG International Journal of Thermal Engineering*, vol. 4, no. 3, pp. 5-7, 2018. [CrossRef] [Publisher Link]

[12] Varchasvi Nandana, and Uwe Janoske, "Numerical Study on the Enhancement of Heat Transfer Performance in a Rectangular Duct with New Winglet Shapes," *Thermal Science and Engineering Progress*, vol. 6, pp. 95-103, 2018. [CrossRef] [Google Scholar] [Publisher Link]

[13] S. Alfarawi, S. A. Abdel-Moneim, and A. Bodalal, "Experimental Investigations of Heat Transfer Enhancement from Rectangular Duct Roughened by Hybrid Ribs," *International Journal of Thermal Sciences*, vol. 118, pp. 123-138, 2017. [CrossRef] [Google Scholar] [Publisher Link]

[14] Hao Wu, David S. K. Ting, and Steve Ray, "The Effect of Delta Winglet Attack Angle on the Heat Transfer Performance of a Flat Surface," *International Journal of Heat and Mass Transfer*, vol. 120, pp. 117–126, 2018. [CrossRef] [Google Scholar] [Publisher Link]

[15] P. Selvakumar et al., "Thermal Plant Condenser Tube Advanced Applied Research on Scale Formation with and Without Magnets in the Water Lines," *International Journal of Engineering Trends and Technology*, vol. 70, no. 5, pp. 173-184, 2022. [CrossRef] [Publisher Link]

[16] Yonggang Lei et al., "Improving the Thermal Hydraulic Performance of a Circular Tube by using Punched Delta-Winglet Vortex Generators," International Journal of Heat and Mass Transfer, vol. 111, pp. 299–311, 2017. [CrossRef] [Google Scholar] [Publisher Link]

[17] Abhay P Asagaonkar, R. D. Shelke, and H. N. Deshpande, "Numerical Investigation of Flow and Heat Transfer Over a Flat Plate using Curved Rectangular Winglet Vortex Generators," *International Journal of Current Engineering and Technology*, pp. 124-128, 2023. [CrossRef] [Publisher Link]

[18] L. H. Tang et al., "A New Configuration of Winglet Longitudinal Vortex Generator to Enhance Heat Transfer in a Rectangular Channel," *Applied Thermal Engineering*, vol. 104, pp. 74-84, 2016. [CrossRef] [Google Scholar] [Publisher Link]

[19] Sombat Tamna, Somchai Sripattanapipat, and Pongjet Promvonge, "Numerical Heat Transfer Study of Turbulent Tube Flow Through Winglet-Pairs," *Energy Procedia*, vol. 100, pp. 518-521, 2016. [CrossRef] [Google Scholar] [Publisher Link]

[20] A. Lemouedda et al., "Optimization of the Angle of Attack of Delta-winglet Vortex Generators in a Plate-fin-and-Tube Heat Exchanger," *International Journal of Heat and Mass Transfer*, vol. 53, no. 23-24, pp. 5386–5399, 2010. [CrossRef] [Google Scholar] [Publisher Link]